Mechanisms involved in the adaptation of Escherichia coli O157:H7 to the host intestinal microenvironment

MECHANISMS INVOLVED IN THE ADAPTATION OF *Escherichia coli* O157:H7 TO THE HOST INTESTINAL MICROENVIRONMENT

Romina J, Fernandez-Brando[1]; Sean P, McAteer[2]; Johanna, Montañez-Culma[1]; Yennifer, Cortés-Araya[3]; Jai, Tree[2,5]; Alan, Bernal[1]; Federico, Fuentes[4]; Stephen, Fitzgerald[2]; Gonzalo E, Pineda[1]; M. Victoria, Ramos[1]; David L, Gally[2]; Marina S, Palermo[1*]

[1]Laboratorio de Patogénesis e Inmunología de Procesos Infecciosos, Instituto de Medicina Experimental (IMEX)-CONICET, Academia Nacional de Medicina, Buenos Aires, Argentina.

[2]Division of Infection and Immunity, The Roslin Institute, University of Edinburgh, Easter Bush Campus, Edinburgh, EH25 9RG, UK.

[3]Division of Functional Genetics and Development, The Roslin Institute, University of Edinburgh, Easter Bush Campus, Edinburgh, EH25 9RG, UK.

[4]Laboratorio de Microscopía, Instituto de Medicina Experimental (IMEX)-CONICET, Academia Nacional de Medicina, Buenos Aires, Argentina.

[5]Current affiliation: School of Biotechnology and Biomolecular Sciences, UNSW, Sydney, Australia.

*** Correspondence:**

Marina S. Palermo

Laboratorio de Patogénesis e Inmunología de Procesos Infecciosos, IMEX

A.P. de Melo 3081

Ciudad de Buenos Aires (C1425AUM),

Argentina

marinasandrapalermo@gmail.com

Tel: 54-11-4809-1050; Fax: 54-11-4803-9475

Keywords: Enterohemorragic *Escherichia coli* (EHEC), Type Three Secretion System (TTSS), host-pathogen interactions, host adaptation, animal model, pathogenicity, transmission intra- and interspecies

Short title: Host adaptation of Stx-producing *E. coli* O157:H7

Clinical Perspective

i. The passage of a clinically isolated EHEC O157 strain (125/99) through the gastrointestinal tract of mice increases its pathogenicity in the same host. In this work, we aimed to elucidate the underlying mechanism(s) involved in the patho-adaptation of this strain.

ii. We demonstrated that the adapted strain has changed the expression of multiple genes involved in various pathogenic mechanisms including: increased adhesion to epithelial cell lines, increased motility on semisolid agar, reduced Stx2 production and increased acid resistance. All these changes led to an improved bacterial fitness in the new host.

iii. Bacterial mechanisms that are required for horizontal transmission of these zoonotic pathogens may overlap with those supporting person-to-person transmission. Understanding how host adaptation modulates the potential virulence of this pathogen is essential for delineating the pathogenesis of disease and may offer novel approaches to prevent and treat EHEC infections.

Abstract

Host adaptation of pathogens may increase intra- and interspecies transmission. We showed previously that the passage of a clinically isolated enterohemorrhagic *Escherichia coli* (EHEC) O157 strain (125/99) through the gastrointestinal tract of mice increases its pathogenicity in the same host. In this work, we aimed to elucidate the underlying mechanism(s) involved in the patho-adaptation of the stool-recovered (125RR) strain. We assessed the global transcription profile by microarray and found almost 100 differentially expressed genes in 125RR strain compared to 125/99 strain. We detected an over-expression of Type Three Secretion System (TTSS) proteins at the mRNA and protein levels and demonstrated increased adhesion to epithelial cell lines for the 125RR strain. Additional key attributes of the 125RR strain were: increased motility on semisolid agar, which correlated with an increased *fliC* mRNA level; reduced Stx2 production at the mRNA and protein levels; increased survival at pH 2.5, as determined by acid resistance assays. We tested whether the over-expression of the LEE-encoded regulator (*ler*) *in trans* in the 125/99 strain could recreate the increased pathogenicity observed in the 125RR strain. As anticipated *ler* over-expression led to increased expression of TTSS proteins and bacterial adhesion to epithelial cells *in vitro* but also increased mortality and intestinal colonization *in vivo*. We conclude that this host-adaptation process required changes in several mechanisms that improved EHEC O157 fitness in the new host. The research highlights some of the bacterial mechanisms required for horizontal transmission of these zoonotic pathogens between their animal and human populations.

Introduction

Enterohemorrhagic Shiga toxin (Stx)-producing *Escherichia coli* (EHEC) O157:H7 has been recognized as the most frequent serotype associated with large outbreaks or sporadic cases of hemorrhagic colitis and hemolytic uremic syndrome (HUS) in many countries [1]. Although the production of Stx determines HUS onset, factors that modulate intestinal colonization are key components in pathogenesis and host mucosal immune response. Among them, there are many fimbrial and non-fimbrial adhesins, flagella, and a type III secretion system (TTSS). Flagella are critical virulence factors not only through permitting bacterial swimming motility but also by promoting adherence to mucins, the major component of the mucus that lines the gastrointestinal tract [2, 3]. The production of Stx (Stx1 and/or Stx2) inhibits protein synthesis in sensitive host-cells and is the principle determinant of renal disease associated with HUS [4]. The locus of enterocyte effacement (LEE) encodes structural and effector proteins of the TTSS, which is also an important virulence factor [5]. The TTSS as well as numerous non-LEE-encoded effector proteins are involved in the colonization process, and allow the modulation of host-cell signaling to favor bacterial replication and survival. Recent work also highlights the importance of Stx for EHEC O157 colonization of cattle [6]. All these virulence factors may contribute to the establishment of infection and subsequent pathology in exposed humans. Virulence gene expression in EHEC is regulated by a number of environmental factors including temperature, culture medium and host-cell factors [7].

Horizontal gene transfer has been shown as a source of genome variability in pathogens not only in infectious disease processes but also in pathogen transmissibility and persistence in a host. This has been demonstrated under homogenous and constant laboratory conditions as well as in complex *in vivo* microenvironments [8, 9]. In the *in*

vivo setting, the multiple specific micro-environments within the same host may force selection for variants involving several mechanisms [10]. Mobile genetic elements, point mutations and genome re-arrangements may facilitate the rapid adaptation of pathogens to changing environmental conditions and hence extend the spectrum of sites that can be infected.

Host adaptation of bacteria has been shown in several pathogens after *in vivo* passage in a host, such as *Corynebacterium pseudotuberculosis* [11], *Helicobacter pylori* [12], *Xenorhabdus nematophila* [13], *Arcobacter butzleri* [14], *Shigella flexneri 2a* [15] and *Salmonella enterica* [16]. These pathogens showed increased capacity to persist in the host, an altered physiology and virulence status favoring infection, when compared with parent strain.

We showed previously that the passage of a clinically isolated EHEC O157 strain (125/99, parent strain) through the gastrointestinal tract of mice increased its pathogenicity in the same host. This stool-recovered strain (125RR) induced a more generalized and persistent colonization than the parent strain, together with the induction of HUS symptoms and mortality with the administration of lower doses than worked out for the parent strain [17]. In the present work, we aimed to elucidate the underlying mechanism(s) involved in the patho-adaptation of this strain to the intestinal environment of mice.

We assessed the global transcription profile by microarray and found almost 100 differentially expressed genes in the 125RR strain. We detected an over-expression of TTSS proteins at the mRNA and protein levels as well as increased adhesion to epithelial cell lines for the 125RR strain. We also detected differences in other known virulence mechanisms between both strains with *in vitro* assays, including motility, acid resistance and Shiga toxin production.

The TTSS is subject to complex control of expression by regulatory networks, often working through the master regulator Ler (LEE-encoded regulator), which is encoded as part of the LEE1 operon [18]. Ler is known to activate TTSS expression by relieving H-NS repression of promoters controlling transcription of multiple LEE operons. Given that 125RR strain had increased expression of TTSS proteins, we asked whether the over-expression of *ler in trans* could emulate the increased pathogenicity observed in the 125RR strain. We observed that *ler* over-expression led to increased mortality and intestinal colonization *in vivo*. These results confirm the central role of TTSS for intestinal colonization and its importance for establishing EHEC O157 infection and pathogenesis.

Our studies have demonstrated that multiple phenotypes have changed in the host-adaptation process leading to improved bacterial fitness in the new host. Even though the mechanisms described herein have been studied previously, this study sheds light on their role in the horizontal transmission of these zoonotic pathogens between their animal and human populations.

Methods

Bacterial strains and media. Bacterial strains used in this study are listed in **Table 1**.

Table 1. Strains and plasmids used in this study.

Strain or plasmid		
Strain	Details	Source
125/99	O157:H7 Stx2, *eae*, clade 8	[19]
125RR	125/99 strain recovered after two consecutive passages through mice	[17]
Δ*stx*	Stx- derivative of 125/99	[20]
Plasmid		
pWSK29	Low-copy number, cloning vector	[21]
pWSK*ler*	IPTG-inducible expression of LEE-	[22]

encoded regulator

Bacteria were cultured in minimal M9 (MM9) medium (6.78 g/L Na_2HPO_4, 3 g/L KH_2PO_4, 1 g/L NH_4Cl, 0.5 g/L NaCl) supplemented with 0.5 % (v/v) glycerol and 2mM $MgSO_4$, Luria-Bertani (LB) broth, trypticase-soy broth (TSB) (Difco, Le Point de Claix, France) or minimal essential medium (MEM)-HEPES (Gibco, Invitrogen San Diego, CA) supplemented with 0.1% (w/v) glucose and 250 nM $(NO_3)_3Fe$. HCT-8 cells were grown in RPMI (Gibco) supplemented with 10 % (v/v) fetal bovine serum (FBS) (Natocor, Córdoba, Argentina), 15 mM L-glutamine (EMEVE, Microvet SRL laboratories, Argentina), and 1 % (v/v) penicillin-streptomycin (EMEVE). Caco-2 cells were grown in DMEM medium (Gibco) supplemented with 10 % (v/v) FBS, 15 mM L-glutamine, 100 mM pyruvate and 1 % (v/v) penicillin-streptomycin. Bacteria harboring pWSK29 or pWSK*ler* plasmids were cultured on media containing 200 µg/mL ampicillin (Bagó, Argentina) in order to help positive selection and avoid plasmid lost.

Microarray analysis. *E. coli* 125/99 and 125RR were cultured overnight in MM9 from single colonies picked from LB plates. The overnight cultures were used to inoculate biological triplicate cultures in 20 mL of M9 medium and incubated at 37°C until growth reached an optical density (OD_{600nm}) of 0.6-0.8. Total RNA was first stabilized and then purified using the RNeasy Protect Bacteria Mini Kit (Qiagen, Hilden, Germany) according to their methods. The samples were treated to remove DNA using an Ambion® DNA-free™ reagent and stored in -80°C. The quality and concentrations of DNAse-treated RNA samples extracted from the two EHEC O157 strains were determined with an Agilent Bioanalyzer (Agilent Technologies, Inc., Santa Clara, CA). Samples were used if the RNA integrity number was between 8-10, with concentrations ranging between 200–500 ng/µL. The expression analysis was outsourced to Edinburgh

Genomics and processed according to the Affymetrix GeneChip Expression Analysis Technical Manual (http://tools.thermofisher.com/content/sfs/manuals/expression_analysis_manual.pdf). Arrays were scanned using a GeneChip® Scanner 3000. The quality of the data with respect to array hybridization, RNA degradation and data normalization was assessed using Bioconductor affycoretools within Bioconductor version 2.1. Differentially expressed genes were determined by applying the 'puma' Bioconductor package [23-25]

Realtime quantitative reverse transcription PCR (qRT-PCR). To verify microarray results, gene expression was examined by qRT-PCR using a Roche Light Cycler and an iTaq™ Universal SYBR® Green Supermix kit (Bio-Rad, Hercules, CA). Primers amplifying 60–140 bp of target genes were designed using Primer-BLAST, NCBI (https://www.ncbi.nlm.nih.gov/tools/primer-blast/) and are listed in **Table 2**.

Table 2. Oligonucleotide primers used in this study

gen		sequence (5'→3')	Source
z3066	F	ACACAATACGGCCAACAGAGA	This study
	R	GTGCACATTGTAACCAGCCA	
ykgO	F	TACCGCAAAAGAACGCCATC	This study
	R	GAACGGCCTTAAAACGTGGA	
espB	F	CAATAAGTTGTTGAATTCCG	This study
	R	TTATACAGCTCCAGATTCCC	
ryhB	F	CGATCAGGAAGACCCTCGCG	This study
	R	AGCCAGCACCCGGCTGGCTA	
ECs1537	F	CATTAACAGAGACCGCAGCC	This study
	R	AAACATCCGGCTTCTTCCAC	
stx2a	F	GAAGAAGATGTTTATGGCGGTTT	[6]
	R	CCCGTCAACCTTCACTGTAA	
escT	F	CGGAAGCGTAAACGCAATCA	This study
	R	TTGTATACTCAGGCCGCTGG	
sepL	F	CGAACGACAGCGCCCTAATA	This study
	R	TGGCGCCTCTTTACTTGACT	
eae			
	F	AGTCGCTTTAACCTCAGCCC	This study
	R	ACTAACTTCCAGTTCCGCCG	
fliC	F	GTGATGCTGCGAAGTCTTA	This study

	R	ACAGAGCCGTTATCCTTGT	
rrsH	F	CGATGCAACGCGAAGAACCT	This study
	R	CCGGACCGCTGGCAACAAA	

185

186 F: Forward primer

187 R: Reverse primer

188 Reaction mixture without template was run as a control. Cycling conditions were as
189 follows: 95ºC for 30 s followed by 40 cycles consisting of 95ºC for 15 s and primer
190 annealing and extension at 60ºC for 60 s. The comparative threshold cycle (CT) ($2^{-\Delta\Delta CT}$)
191 method was used to analyze the relative transcription levels of target genes as described
192 previously [26]. The housekeeping gene *rrsH* was used as a reference for normalization
193 of samples. RNA was prepared from three independent cultures and qRT-PCR
194 measurements were run at least 2 times for all samples.

195 **Analysis by SDS-Page of TTSS culture supernatant proteins.** Bacteria were cultured
196 overnight in MM9 or MEM-HEPES supplemented with glucose and Fe^{3+} and diluted
197 1/100 in the same medium the following day to an optical density of 600 nm (OD_{600})
198 ~0.9. pWSK*ler* and pWSK29 transformed bacteria were grown for 1 h when 1 mM of
199 isopropyl β-D-1-thiogalactopyranoside (IPTG) (Sigma-Aldrich, San Luis, MO) was
200 added and bacteria were grown for 4 additional hours. Samples were prepared from
201 equal volumes of bacterial culture (25 mL) on the indicated media. Cultures were
202 centrifuged at 4000 *g* for 30 min and supernatants passed through a 0.45 µm low-
203 protein-binding filter (Millipore, Burlington, MA). Trichloroacetic acid [TCA] (Sigma-
204 Aldrich) was added at a final concentration of 10 % (v/v) together with 4 µg/mL bovine
205 serum albumin [BSA] (NEB, Ispwich, MA) in order to precipitate proteins at 4°C
206 overnight. Then, solutions were centrifuged at 4000 *g* for 30 min at 4°C and
207 supernatants were poured off carefully. Protein pellets were sequentially air-dried, re-
208 suspended in 0.004 volumes of 1.5 M Tris-HCl pH 8.8 and separated through a 12 %

SDS-PAGE, which was stained with Colloidal blue (Severn Biotech, UK). Gel images were obtained by using a Flowgen MultiImage light cabinet and ChemiImager 4000i v.4.04 software.

Western blotting. EspD and RecA were analyzed by western blot as previously described [27]. Briefly, supernatant proteins were obtained and separated through a 12% SDS-PAGE as above. Cell pellets from 1 mL of the same cultures were centrifuged, suspended in 0.1 mL 2x Laemmli buffer and incubated at 100°C for 5 min. Proteins were then separated through a 10% SDS-PAGE and transferred onto Hybond ECL nitrocellulose membrane (GE Healthcare Life Sciences, Marlborough, MA) using a Trans-Blot electrophoretic transfer cell (Bio-Rad). After membranes were blocked with 5% (w/v) milk powder (Sigma) in phosphate buffered saline (PBS) at 4°C overnight, were sequentially incubated with 1:2,000 mouse monoclonal anti-EspD (Gift from Prof. Trinad Chakraborty, University of Giessen) or 1:10,000 anti-RecA (Enzo Life Sciences, Farmingdale, NY) and then 1:3,000 rabbit polyclonal anti-mouse IgG-HRP conjugated antibodies (NEB), all diluted in PBS containing 5% (w/v) milk powder. Incubations were carried out at room temperature for at least 1 h on a platform shaker and were washed for 3 x 5 min in PBS before and after each antibody step. Membranes were visualized with chemiluminescent detection (GE Healthcare Life Sciences) on Hyperfilm ECL film (GE Healthcare Life Sciences) developed in a Protec automatic film processor (Optimax, Germany). Images were taken as above. Bands were quantified by using ImageJ as follows. The area of each individual band was delimited and the raw intensity density was measured. This value was corrected by subtracting the background intensity of an equivalent area to each individual band and expressed as Arbitrary Units. The mean ratio between EspD and RecA intensity was calculated from three repeats.

Cell binding assays. 2 x10^5 Caco-2 cells or 4x10^5 HCT-8 cells per well were seeded into 12 well plates (GBO, Germany) and incubated overnight. The following day, 1 h before bacteria were added, cell cultures were washed twice with PBS and 500 µL of MM9 or MEM-HEPES supplemented with glucose and Fe^{3+} per well was added. Parent (125/99) and stool-recovered (125RR) strains were cultured 24 h in MM9, sub-cultured (1:100) into pre-warmed MM9 at 37ºC 200 rpm for 2 h, and 200 µL of each bacterial suspension added by triplicate to Caco-2 and HCT-8 cell cultures (MOI≈ 5 and 20 respectively). Recombinant bacteria (125/99 pWSK*ler*, 125/99 pWSK29, Δ*stx* pWSK*ler* and Δ*stx* pWSK29) were cultured overnight in LB medium supplemented with 200 µg/mL ampicillin, sub-cultured (1:100) into pre-warmed MEM-HEPES medium supplemented with ampicillin, glucose and Fe^{3+} at 37ºC 200 rpm for 1 h, 1 mM of IPTG was then added in order to induce *ler* expression and cultured for 4 additional hours. Bacterial suspensions were diluted 1/20 dilution in the same medium and 200 µL of each bacterial suspension was added in triplicate to Caco-2 and HCT-8 cell cultures (MOI≈10). A low speed centrifugation (1000 x g for 5 min) was carried out in order to synchronize bacterial adhesion and bring all the bacteria directly in contact with the cells [28]. Cells were incubated at 37°C in 5 % CO_2 in a moist box for 4 h. Supernatants containing non-adherent bacteria were discarded, cells were washed five times with sterile PBS and 200 µL of sterile PBS containing 0.1 % Triton X-100 was added. Cells on each well were scraped off, suspensions serially diluted 1/10 in PBS, and triplicate plated onto LB plates containing 200 mg/mL ampicillin when necessary. The plates were incubated overnight at 37°C, and colonies were counted the next day. For microscopy analysis, epithelial cells were seeded onto sterile glass coverslips pre-coated with rat collagen I (Gibco) according to manufacturer's instructions. Bacteria were cultured as indicated above and incubated with cells for 1 h by duplicates, when cells were washed twice with PBS, and incubated for 3 or 4 more hours. After this time, cells

were fixed using fresh 4 % paraformaldehyde (PFA) for 30 min, permeabilized with 2 % PFA containing 0.25 % Triton X-100 at room temperature for 10 min and blocked with PBS containing 5 % BSA at room temperature for 1 h. After three washes with PBS, infected cells were incubated overnight with mouse anti-lipopolysaccharide (LPS)-O157 antibody (Abcam, UK) at 1:2,000. After three more washes, samples were incubated with Alexa Fluor 488-conjugated goat anti-mouse immunoglobulin antibody at 1:200 (Molecular Probes, Oregon, USA) for an hour. Staining of F-actin was carried out with Phalloidin iFluor-555 at 1:1,000 (Abcam) and nuclei were stained with TO-PRO 3-iodide at 1:500 (Thermo Fisher Scientific) for 40 min at room temperature. Slides were washed three times with PBS, mounted with ProLong™ Diamond Antifade (Thermo Fisher Scientific) and coverslips were applied. Image acquisition was performed by using a FluoView FV1000 confocal microscope (Olympus, Tokyo, Japan) equipped with a Plapon 60X/1.42 objective. Images were analyzed with ImageJ software (NIH) and fluorescence was quantitated.

Automated Image Analysis. Images were analyzed using Fiji software and macros for automatized image quantification were designed. A threshold was applied to the maximum image projections (MIPs) of the bacteria corresponding channel and regions with an area over 400 nm^2 were considered for analysis. MIPs of the actin signal were obtained and a low threshold was applied in order to include the whole cell area for the generation of a mask. The mask was applied to the bacterial positive regions and the bacterial area was measured. The number of cells per image was obtained by counting the nuclei. Data was expressed as bacterial area per nucleus.

Motility assays. Motility assays were conducted on motility soft agar plates as previously described [29]. Motility plates were made with 0.3 % (w/v) agar, 1 % Tryptone and 0.25 % sodium chloride, and allowed to dry for 1 h in a biological safety

cabinet before being inoculated. Each strain was cultured for 24 h on MM9 media as indicated and a 4 µL aliquot was spotted by triplicate nearly the center of a motility plate. Motility was detected visually and diffusion halos were measured after 24 and 48 h of growth at 37ºC.

ELISA. Ninety-six-well microtiter plates (GBO, Germany) were coated by incubating overnight with 5 µg/mL anti-Stx2 per well in 15 mM carbonate, 25 mM bicarbonate (pH 9.6) at 4ºC. Then, 200 µl of PBS containing 5 % BSA was added to each well and the plates were incubated for 2 h at room temperature. The plates were washed three times with PBS containing 0.05 % Tween 20 and incubated for 2 h at room temperature with 50 µL of the supernatant of each culture by duplicate. As control for the unspecific binding, the culture supernatant of isogenic Δ*stx* derivative of 125/99 (Δ*stx*) [20] was added. After three washes, the plates were incubated 2 h at room temperature with 50 µL of mouse polyclonal anti-Stx2 diluted 1:1,000 in PBS containing 0.05 % Tween 20 and 1 % BSA. After three washes, the plates were incubated 2 h at room temperature with 50 µL of goat anti-mouse horseradish peroxidase-conjugated (BioRad) diluted 1:3,000 in PBS containing 0.05 % Tween 20 and 1 % BSA. After three more washes, 50 µL of substrate solution (0.1 M citrate-phosphate pH 5, 1 mg/mL o-phenylenediamine dihydrochloride [OPD] (Sigma-Aldrich), 30 % H_2O_2) was added to each well and incubated for 20 min at room temperature in the dark. The reaction was stopped by the addition of 50 µL of 4 N sulfuric acid and the optical density values at 492 nm (OD_{492}) were measured in a microplate ELISA reader (Microwell System Reader 230s, Organon, Teknika, OR). In order to quantify the Stx2 concentration a standard curve was carried out with recombinant Stx2 (Phoenix lab, Tufts University, Boston, Mass., USA). The mean Stx2 concentration ± SEM was calculated.

Acid stress assays. The effect of brief acute acid stress on 125/99 and 125RR strains was investigated. The method used to assay acid survival was similar to that described by Bak et al [30]. All cultures were at 37°C with shaking at 200 rpm. Bacteria were grown for 24 h in MM9 media and diluted 1/10 (30 µL of bacteria (approximately 10^8 CFU in 270 µL of the respective media in 1.5 mL Eppendorf tubes) the following day into MM9 media adjusted to pH 2.5 with HCl and supplemented as follow in order to study the different acid resistance (AR) mechanisms. To study AR0 the overnight culture were grown in MM9 media supplemented with 0.4 % glycerol and acid challenged in MM9 media supplemented with 0.4 % glucose. To test AR1 and AR2 overnight cultures were grown in MM9 media supplemented with 0.4 % glucose and acid challenge was carried out in the presence of 1.5 mM glutamate or 0.6 mM arginine respectively. Bacteria were exposed to a pH 2.5 for 1 and 2 h. Samples were taken at time 0 and at 1 and 2 h of acid stress, and serial dilutions were done, plated onto LB agar plates and incubated at 37°C in order to calculate the percentage of survival after the acid stress. Cell survival was determined in triplicate and their values were given as a mean average. Survival percentage was calculated as 100 × the number of CFU/mL remaining after the acid treatment divided by the initial CFU/mL at time zero.

Mouse infection. The transformed strains were cultured in TSB containing 200 µg/mL ampicillin to mid-exponential phase, diluted 1/100 in the same medium and cultured at 37°C 200 rpm overnight. Cultures were centrifuged at 4000 *g* for 30 min at 4°C, supernatants removed and bacterial pellets washed twice in PBS. Bacteria were diluted to reach the desired final concentration and further serially diluted 1/10 and spread onto LB agar plates containing ampicillin to determine the number of CFU/mL.

C57BL/6 male and female mice were maintained under specific-pathogen-free conditions in the animal facility of the Instituto de Medicina Experimental, Consejo

Nacional de Investigaciones Científicas y Técnicas, Academia Nacional de Medicina, Buenos Aires, Argentina. The experiments described here were approved by the Institutional Animal Care and Use Committee (protocol 40/2017) in accordance with the principles set forth in the Guide for the Care and Use of Laboratory Animals [31]. Mice were housed in standard transparent polypropylene cages under environmentally controlled conditions (temperature, 24±2°C; humidity, 50±10 %) with a 12 h light-dark cycle. Mouse infection was as previously described [19]. Basically, mice were weaned (16-19-days old, approximately 6-9 g of weight), divided randomly into experimental groups and starved for at least 4 h. One-hundred µl of each bacterial suspension was delivered directly into the stomach via a stainless steel cannula (model 7.7.1, 0.38-mm outside diameter, 22 gauge; Harvard Apparatus, Cambridge, MA). After bacterial administration both food and water were provided to mice *ad libitum*.

Monitoring mouse infection. Animals were observed daily for activity level and water intake up to 8 days, when survivors were euthanized. At 96 h after infection blood samples were obtained by puncture of the retro-orbital plexus under isoflurane anesthesia. To assess renal compromise, urea plasma concentrations were determined by an enzymatic-colorimetric kit in accordance with the manufacturer's instructions (Wiener Lab, Rosario, Argentina). All moribund mice were humanely euthanized according to IACUC guidelines to define humane endpoints. Survival analyses were performed with inoculated animals.

Colonization: isolation and enumeration of EHEC strains from mouse intestine. Mice were killed at 96 h after bacterial inoculation to determine intestinal colonization as previously described [19]. In brief, small and large intestines were excised and the stool was removed, diluted to 1 g/mL and plated onto SMAC and LB agar plates containing 200 µg/mL ampicillin to determine the number of CFU per gram of feces.

Each segment of the intestine (5 cm each) was washed vigorously with sterile PBS and homogenized in 0.5 mL PBS, serially diluted and plated onto SMAC and LB agar plates containing 200 μg/mL ampicillin and incubated overnight at 37°C. The non-sorbitol fermenting ampicillin resistant colonies were counted. The number of CFU per intestinal section was calculated multiplying the CFU/mL by the total volume of each sample. SMAC and LB agar plates gave equivalent CFU counts.

Statistical analysis

Data are expressed as mean ± standard error of mean (SEM) and were analyzed for statistical differences either by two-tailed Student's t-test or one or two-way analysis of variance (ANOVA) according to the number of experimental groups. ANOVA analyses were followed by a comparison between treatments performed by the Bonferroni Multiple Comparison test. Survival curves were analyzed by Log-rank Test. A confidence level of >95% ($P<0.05$) was considered as significant.

Results

Analysis of global gene expression

To understand the differences that could explain the increased pathogenicity observed in the stool-recovered (125RR) strain we carried out a global analysis of gene expression by using high-throughput DNA microarrays. The expression of each gene was normalized to its expression in the parent strain (125/99). **S1Table** shows the top one-hundred genes that were differentially expressed by the 125RR strain compared to the 125/99 strain. Genes were grouped according to their function in categories by using the EcoCyc database [32] and the annotated sequence of *E. coli* O157:H7 EDL 933 [33]. Categories included: membrane/transport, phosphonate metabolism, amino acid

biosynthesis, protein metabolism, virulence, DNA integration/transposition, sRNAs, bacteriophage/prophage related and hypothetical.

There was increased expression of several genes encoding specific transport systems and pathways for protein and phosphate metabolism, as well as some virulence determinants (**S1 Table**). For example, among the 11 differentially expressed transport-related genes, 8 genes (73%) were up- and 3 (27%) down-regulated. Several of them were involved in metal binding, especially iron (*fepA*, *fiu*, *yciF*) and zinc (*zinT*, *znuA*), as well as for heme/hemoglobin (*chuA*). In addition, 3 (43%) out of 7 genes related to virulence were up-regulated in their expression. Among them, we found *espB*, encoding part of the type three-secretion system (TTSS) translocon complex and *pliG*, an inhibitor of g-type lysozyme. Among the down-regulated genes, there were two encoding secreted effector proteins (*espN*, *espX7*) as well as *ECs0621/Z0722*, encoding HokE from a toxin-antitoxin system.

Several genes had reduced expression levels; hypothetical proteins accounted for 23 (25%) of these, 17 (18%) were defined as bacteriophage/phage-related genes, 15 genes (16%) as sRNAs, 9 genes (10%) as DNA integration/transposition and 4 genes (4%) linked to amino acid biosynthesis. In addition, 3 genes grouped as membrane/transport were also down-regulated: *narK*, a nitrite/nitrate antiporter; *dppB*, a putative subunit for dipeptide transport system permease; and *btuC*, a vitamin B12-transporter permease.

Among the down-regulated sRNAs, *rprA*, *arcZ* and *dsrA* have been shown to be involved in the stabilization of RpoS mRNA, encoding the general stress sigma factor [34]; and *spf* (Spot 42 sRNA), which has been shown to directly repress translation of SepL the first protein expressed on LEE4 that encodes the TTSS translocon complex [35].

Quantitative RT-PCR

To confirm the results obtained by microarray and study the expression of several genes important for EHEC pathogenesis, qRT-PCR was conducted. The relative expression ratio of the genes of interest was calculated using the $2^{-\Delta\Delta CT}$ formula described previously [26]. The reference gene was the ribosomal gene *rrsH*.

To confirm the microarray assay, we selected the genes *z3066* ($\log_2$FC=2.07) and *ykgO* ($\log_2$FC = 2.25) that were up-regulated and *ryhB* ($\log_2$FC = -0.83) and *ECs1537* ($\log_2$FC = -0.85) that were down-regulated, since they showed the highest differential expression with statistical significance ($p<0.05$). Expression of the selected genes by qRT-PCR showed results that were consistent with the microarray (**Fig 1**).

Although EspB, a critical component of the TTSS injectosome, only showed a marginal p value (0.06) and a $\log_2$FC= 0.95, it was included in qRT-PCR analysis given its central role of TTSS proteins on colonization. We observed the same trend on the expression level of EspB by qRT-PCR as that observed on the microarray (**Fig 1**). The TTSS is encoded by the locus of enterocyte effacement (LEE) pathogenicity island that is formed of 5 operons, which encode the injection apparatus and several secreted effector proteins. EspB/D are both encoded on LEE4 and form the pore structure in the host cell membrane through which effector proteins are injected. The expression of several genes from LEE pathogenicity island were analyzed by qPCR (**Fig 1**), *escT*, *sepL* and *eae*, from LEE1, 4 and 5 respectively. We observed that all these LEE genes had higher expression in the 125RR than the 125/99 (**Fig 1**), even though the expression levels were not significantly different by microarray. In this regard, it has been reported that discrepancies between qRT-PCR and microarray could be due to the higher sensitivity of the qRT-PCR together with the higher efficiency of the retro-transcription step in qRT-PCR reactions, since there is no dye incorporation [36].

Quantitative RT-PCR analyses also demonstrated that *stx2* had reduced expression, while *fliC* was over-expressed in the125RR strain (**Fig 1**).

Expression of TTSS proteins

As we observed increased *espB* mRNA levels by both microarray and qRT-PCR as well as increased mRNA levels of *escT*, *sepL* and *eae* in the 125RR strain, we analyzed production of the T3SS translocon by Western blotting for EspD. Both strains were cultured in the same medium used in the microarray and qRT-PCR assays (MM9) and EspD was evaluated in the supernatants. As **Fig 2A-B** show we observed significantly increased EspD expression for the 125RR strain compared to 125/99 strain, in agreement with the microarray and qRT-PCR results.

To assess if the increased expression of several TTSS genes as well as EspD protein was associated with changes in adherence to epithelial cells *in vitro*, 125/99 and 125RR strains were cultured in MM9 medium and applied to monolayers of HCT-8 and Caco-2 epithelial cells as described in the Methods section. There was a significant increase in the percentage of 125RR bacteria that adhered to both epithelial cell lines compared to 125/99 strain (**Fig 2C**). We confirmed these results by quantifying numbers of bacteria relative to nuclei using confocal microscopy (**Fig 2D-E**).

Collectively, an increased mRNA level of TTSS genes, together with increased expression of EspD were observed for the 125RR compared to 125/99 strain and this correlated with increased bacterial adhesion to HCT-8 and Caco-2 epithelial cells.

Phenotypic changes in other known virulence mechanisms

***fliC* expression and motility.** Since we found that *fliC* was significantly over-expressed in the 125RR strain (**Fig 1B**), we tested bacterial motility in soft agar plates. Motility

halos were measured at 24 and 48 h. We found significantly increased swimming motility at 48 h for the 125RR strain compared to the 125/99 strain (**Fig 3A-B**), thus supporting the qRT-PCR result at a functional level.

Shiga toxin expression. We confirmed that the stool-recovered strain had a significantly reduced Stx2 production at the mRNA (**Fig 1B**) and protein (**Fig 3C**) level compared to the parent strain.

Acid resistance. As we detected a differential expression of three sRNAs, *arcZ*, *dsrA* and *rprA*, that are known to be involved in regulating the response to several stresses through the stationary phase sigma factor [34], we tested the acid resistance (AR) of 125/99 and 125RR strains.

There are three AR systems in *E. coli* that can be classified as amino acid dependent or independent. The amino acid dependent include AR1 or glutamate-dependent and AR2 or arginine-dependent. The amino acid independent or AR0 or oxidative is repressed in the presence of glucose [37]. Thus, in order to study these mechanisms we cultured the parent and stool-recovered strains in MM9 medium overnight. The following day the bacteria were exposed to pH 2.5 for 1 and 2 h and percent survival determined as described in the Methods section.

We observed that the 125RR strain had a significantly increased survival after 1 and 2 h of acid stress in the different conditions set to evaluate AR0-2 (**Fig 3D-E**).

ler over-expression affects TTSS expression, bacterial motility and Stx production

TTSS is subject to complex control of expression by regulatory networks, often working through the master regulator Ler, which is encoded as part of the LEE1 operon and helps activate transcription of multiple TTSS operons [18]. Since we observed that the

125RR strain had increased TTSS protein expression, we wanted to test if *ler* over-expression in the 125/99 strain would mimic the same host adaptation and pathogenic effect as determined for 125RR as a result of serial passage through the murine gastrointestinal tract. To this end, we transformed the 125/99 strain with a plasmid containing the *ler* sequence under control of an IPTG-inducible promoter (pWSK*ler*). In addition, we transformed the isogenic Δ*stx* derivative of 125/99 [20] with pWSK*ler*, to further analyze cross-regulation between *stx* and *ler* (Δ*stx* pWSKler). The plasmid without the *ler* sequence was used as a control (pWSK29) [21] in both strains 125/99 (125/99 pWSK29) and the isogenic Δ*stx* (Δ*stx* pWSK29).

First, we checked if expressing *ler in trans* leads to increased expression of TTSS proteins. Both strains transformed with pWSK*ler*, 125/99 and Δ*stx*, showed increased expression of EspB/D compared to the strains containing the pWSK29 plasmid (**Fig 4A**). Besides, *ler* over-expression resulted in increased adhesion to Caco-2 epithelial cells compared to strains with no *ler* over-expression (125/99 pWSK29 and Δ*stx* pWSK29) (**Fig 4B**). This effect was confirmed by confocal microscopy (**Fig 4C-E**), in which *ler* over-expressing strains showed typical actin condensation beneath adherent bacteria, characteristic of attaching and effacing (A/E) lesions (**Fig 4D**). Both *ler* over-expressing strains, 125/99 and Δ*stx*, showed similar adhesion levels, and the absence of *ler* over-expression in the Δ*stx* strain (Δ*stx* pWSK29) resulted in significantly lower adhesion to epithelial cells than the presence of *stx* and *ler* over-expression (125/99 pWSK*ler*) (**Fig 4C-E**). Next we analyzed the effect of *ler* over-expression on Stx production. Stx2a released to the culture media was measured at different times following *ler* induction (**Fig 4F)**. Stx production was significantly increased at 3.5 h of *ler* induction for the125/99 pWSK*ler* strain.

503 We also evaluated bacterial motility in these strains. *ler* over-expression reduced
504 motility, since both pWSK*ler* containing strains showed lower motility than the
505 respective pWSK29-transformed strain (**Fig 4F**).

506 **Increased *ler* expression increases pathogenicity *in vivo***

507 Finally, we tested the capacity of these strains to colonize and induce the pathological
508 outcomes of EHEC infection in the weaning mouse model described previously [19].
509 We inoculated mice with the different strains and evaluated survival, plasmatic urea
510 levels and intestinal colonization (**Fig 5A-E**). As **Fig 5A** shows, 125/99 pWSK*ler* strain
511 showed the highest lethality for mice, as none (0/10) of 125/99 pWSK*ler* inoculated
512 mice survived longer than 96 h following inoculation while 40% (4/10) of 125/99
513 pWSK29 inoculated mice survived. Animals in which EHEC infection led to death
514 showed weight loss, ruffled fur, hunched posture, shivers and decreased activity
515 including lethargy and ataxia. In addition, the increased plasmatic urea levels for mice
516 inoculated with 125/99 pWSK*ler* strain supported the characteristic Stx-associated renal
517 failure observed in moribund mice (**Fig 5B**). Since 40% of mice inoculated with 125/99
518 pWSK29 survived and showed normal urea levels but mice that die showed high urea
519 levels, this group showed an intermediate mean urea level. As expected, mice
520 inoculated with Δ*stx* pWSK*ler* and Δ*stx* pWSK29 showed 100% survival and normal
521 urea levels. In order to investigate if the increased mortality observed in 125/99
522 pWSK*ler* inoculated mice was related to increased adherence to intestinal epithelium,
523 we evaluated intestinal colonization of inoculated mice at 96 h, before 125/99 pWSK*ler*
524 inoculated mice died (**Fig 5A**). The 125/99 pWSK*ler* strain was recovered from small
525 and large intestine of inoculated mice in higher amounts than Δ*stx* strains (Δ*stx*
526 pWSK*ler* and Δ*stx* pWSK29) (**Fig 5D and E**). Δ*stx* pWSK*ler* and 125/99 pWSK29
527 showed similar CFU numbers in both intestinal segments. On the other hand, bacterial

528 recovery from feces was similar in Δ*stx* pWSK*ler* and 125/99 pWSK*ler* inoculated mice
529 (**Fig 5C**).The Δ*stx* pWSK29 strain showed significantly lower CFU numbers in all the
530 samples compared to 125/99 pWSK*ler*.

531

532 Discussion

533 In this work, we have investigated mechanisms by which an EHEC O157 strain subject
534 to repeated passage through the mouse intestinal tract has increased pathogenesis. This
535 work identified for the first time factors important during host adaptation that lead to
536 increased virulence of EHEC O157.
537 We showed that the stool-recovered strain (125RR) had changed levels of expression
538 for nearly 100 genes, some of which were confirmed at the protein and functional level.
539 We showed that increased expression of TTSS by the 125RR strain mediated increased
540 bacterial adhesion to epithelial cells. Additionally, the 125RR strain showed increased
541 motility, reduced Stx2 production and increased survival at pH 2.5. We propose that
542 these mechanisms in combination allow the 125RR strain to facilitate higher levels of
543 Stx entry through the intestinal epithelium to the systemic circulation resulting in more
544 severe Stx-induced pathology in the host with a lower infective dose than the parent
545 strain. This is in spite of the fact this strain *in vitro* produces less Stx than the parent
546 strain. Even though this screen generally identified established virulence factors, the
547 study has highlighted their role for horizontal transmission of this zoonotic pathogen
548 between different host species.
549 The use of microarrays has the advantage of allowing the simultaneous measurement of
550 expression across the bacterial genome in a single hybridization assay [38]. It is
551 appreciated that data obtained by this technique represents a snapshot of the

552 physiological state of the sample at a single time point that will not reflect the whole
553 story, since bacteria adapt constantly to changing environments and express virulence
554 factors in a hierarchical manner. In addition, a large proportion of the gene products
555 identified encode hypothetical proteins [39, 40]. In this case, 33 out of 92 (36%) of the
556 differentially expressed genes encode hypothetical proteins and some may be important
557 for the disease processes and should be further investigated.

558 Among the up-regulated genes in the 125RR strain were several membrane/transport
559 proteins (9%), some of which were involved in transport of iron (*fepA*, *fiu*, *yciF*),
560 heme/hemoglobin (*chuA*) and zinc (*zinT*, *znuA*). It is well established that iron
561 acquisition is essential to the survival of every organism, including intestinal pathogens
562 that must compete for it with the host and other commensals. Additionally, dietary heme
563 is abundant in this milieu and thus an important iron source [41]. In this regard, the
564 increased expression of proteins involved in iron and heme acquisition in the stool-
565 recovered strain may be advantageous for this niche occupation and gut colonization.
566 On the other hand, *zinT* is required for maintaining intracellular zinc concentration in
567 EHEC in conditions of zinc deficiency, while *znuA* contributes to zinc recruitment in
568 the periplasmic space, thus facilitating bacterial adhesion to epithelial cells [42]. These
569 observations could imply that the ability of bacteria to compete with the host cells for
570 zinc binding is also critical to establish a successful infection. Among the virulence
571 genes, *pliG* was found to have higher expression levels. The protein inhibits g-type
572 lysozyme [43], thus *pliG* over-expression could help to defend bacteria against the lytic
573 action of host lysozymes. Collectively, these observations from the 125RR strain
574 revealed different classes of proteins involved in distinct mechanisms that could
575 contribute to the competition with commensals and the infectious process of this
576 pathogen.

577 The differential expression of Type Three Secretion System (TTSS) by the 125RR
578 strain was another novel finding of this work. In fact, *escT* from LEE1, *espB/D* and
579 *sepL* from LEE4, and *eae* (intimin) from LEE5 were found to be expressed at higher
580 levels than the parental strain by microarray and/or qRT-PCR. The lower expression of
581 *spf* encoding the Spot42 sRNA concurs with this finding, since Spot42 was found to
582 repress translation of LEE4 [35]. Although EscT and EspB are both structural
583 components of the injectosome, EscT is a component of the basal apparatus while EspB
584 helps form the translocation pore with EspD in the eukaryotic host cell. SepL is a
585 cytoplasmic component involved in the regulation of effector secretion, and Intimin is
586 the protein that adheres to its translocated receptor, Tir, thus enabling intimate
587 attachment [44]. The increased expression of TTSS components by 125RR was
588 associated with increased adhesion to gut epithelial cell lines (HCT-8 and Caco-2).
589 Intestinal colonization is the first step in the infection process and it was postulated that
590 the degree of gut adherence may correlate with the ability to cause disease and induce
591 systemic Stx-mediated pathology [45]. Besides, gut adherence is also a factor that
592 distinguishes human-virulent from non-virulent Stx-producing *E. coli* strains found in
593 contaminated food [46] or cattle [47]. In addition, it was shown that EHEC strains
594 colonize the intestine through a finely regulated process that involves the sequential
595 expression of flagella and TTSS [2], and the 125RR strain also had an increased
596 expression of *fliC*, the major structural subunit of the flagellar filament, and exhibited
597 increased motility on soft agar plates. Flagella expression and motility enable bacteria to
598 overcome the mucus barrier that covers intestinal epithelial surfaces in order to reach
599 the epithelial cell surface. The role of the motility mediated by flagella for virulence has
600 been studied extensively. Mahajan *et al*., 2009 have shown that flagella mediate initial
601 adhesion to epithelial cells *in vitro* and *in vivo* during colonization of the bovine
602 intestine **[2].** More recently, the initial interactions among flagella, host cell membranes

603 and cytoskeletal components have been described **[3].** Besides, flagella and the TTSS
604 demonstrate cross-regulation [48] and our findings showed that both TTSS and flagella
605 expression were increased in the 125RR strain potentially promoting mucus layer
606 penetration followed by TTSS subversion of host cells.

607 Although some studies have associated greater pathogenic potential of STEC with
608 increased Stx2 production [49], 125RR strain produced less Stx2a but increased
609 pathology than the parent strain. These results are in line with Olavesen's report [50],
610 which showed that an EHEC O103:H25 strain, isolated from HUS patients during a
611 nationwide outbreak in Norway in 2006, had a 60% HUS frequency and the expression
612 level of Stx2 mRNA *in vitro* was low. Even if Stx2 production *in vivo* is lower for the
613 125RR strain, these findings indicate that other factors work in concert with Stx
614 production and are important for EHEC disease severity [51].

615 The 125RR strain was also demonstrated to have an increased resistance to acid stress,
616 most importantly using the amino acid independent or glucose-repressed AR0
617 mechanism but also the glutamate-dependent AR1 and arginine-dependent AR2
618 mechanisms. This increased acid resistance agrees with the previous observation that
619 125RR strain is infective even when it is administrated in small doses in a mouse model
620 of HUS [17]. Food-borne pathogens must survive in pH values as low as 1.5–2.5 in the
621 stomach in order to establish an infection. This ability to tolerate acidity probably does
622 contribute to its low infectious dose (50–100 organisms) [52]. The AR systems have
623 been extensively studied in EHEC [37]. Environmental conditions such as media
624 composition, bacterial growth phase, aerobic or anaerobic conditions, presence of
625 specific amino acids and challenging pH, determine the induction of a specific AR
626 system. In the absence of mild acid stress, the AR0-AR2 systems are the mechanisms
627 used to resist acid stress and depend on RpoS [53], the expression of which is initiated

during the transition phase between exponential and stationary-phase and continues to high levels in stationary-phase [34]. In agreement with this, 125RR cultured to stationary-phase in MM9 medium had increased resistance to pH 2.5 by using AR0-2. The three AR systems were shown to depend on RpoS in some extent [30], and RpoS was shown to induce GadX, a global regulator of AR, as it controls the majority of genes found in the acid fitness island (AFI) [54]. Although the mechanism underlying AR0 is not well understood yet, AR1 has many regulators that depend on growth conditions. Glutamate decarboxylases, GadA and GadB, are key enzymes for the AR1 system and are induced after the RpoS-dependent expression of GadX and subsequently GadE in stationary-phase cells [55].

Given that the increased expression of TTSS proteins could explain the greater colonization of mouse intestine of 125RR strain, we tested this hypothesis by transforming the 125/99 strain with a plasmid containing the *ler* sequence down-stream of an IPTG-inducible promoter (pWSK*ler*). The LEE island is subject to multiple regulatory mechanisms [7, 22], often acting through the LEE-encoded regulator (Ler) [18], which is encoded in the LEE1 operon. Ler is known to activate TTSS protein expression by lifting H-NS repression [56]. We observed that two *ler* over-expressing strains (125/99 Stx+ and Δ*stx* pWSK*ler*) showed a similar increased expression of TTSS proteins, as well as increased adherence to epithelial cells compared to the strains with no *ler* over-expression (125/99 Stx+ and Δ*stx* pWSK29). In this sense, *ler* over-expression seems to have a more predominant role than Stx expression in adherence in the *in vitro* setting, given that both *ler* over-expressing strains showed similar adhesion levels both higher than the respective strains with no *ler* over-expression. In contrast, Stx expression seems to contribute to *in vivo* colonization, since 125/99 pWSK*ler* showed significantly higher colonization in small and large intestines than Δ*stx*

653 pWSK*ler*, and 125/99 pWSK29 showed similar levels of adhesion to intestinal epithelia
654 than Δ*stx* pWSK*ler*. Setting aside the differences between human and mice, *in vivo*
655 intestinal colonization exposes EHEC to a complex set of microenvironments including
656 a mucus layer and competition with microbiota for nutrients and niche occupancy prior
657 to epithelial colonization,. In line with our findings, it was previously shown in the
658 mouse model that Stx expression during colonization leads to a redistribution of
659 nucleolin, a eukaryotic receptor that binds Intimin and promotes bacterial attachment
660 [57]. More recently, it has been shown that Stx2a and 2c can inhibit proliferation of
661 bovine gut enteroids providing another way that Stx can promote adherence and
662 persistence on the epithelium [6]. In agreement with both findings, we observed that Stx
663 increased bacterial adhesion *in vivo* when TTSS is over-expressed in 125/99 pWSK*ler*
664 strain, which also reduced mouse survival. Given that there is a cross-regulation among
665 TTSS, flagella and Stx, and this regulation contributes to the hierarchical expression of
666 factors to improve colonization, we analyzed motility and Stx expression in these
667 bacteria. We observed that *ler* over-expression reduced swimming motility in soft agar
668 plates, which was further reduced in the presence of Stx, since the 125/99 pWSK*ler*
669 strain showed the lowest motility. This observation is in agreement with previous
670 findings showing that GrlA is a key regulator involved in the reciprocal regulation of
671 flagella and the TTSS [58], and is positively regulated by Ler [59]. It was suggested that
672 this regulation might be important for efficient cell adhesion by EHEC, since flagella
673 might sterically hinder interaction of TTSS apparatus with the epithelium [2, 58]. Even
674 when the 125/99 pWSK*ler* strain showed the lowest motility *in vitro*, it did not have a
675 negative impact on colonization *in vivo*, since 125/99 pWSK*ler* strain had the highest
676 adherence levels to mouse intestine.

Finally, we observed that the strain over-expressing *ler* produced higher amounts of Stx than the isogenic strain with no *ler* over-expression. A connection between Stx and TTSS production through the SOS response has been reported, since both pathogenic factors are up-regulated by DNA damaging agents [56]. Stx is encoded on the late lytic region of lambdoid phages [60], and DNA damage leads to the autocatalytic cleavage of the CI repressor promoted by activated RecA, and transcription of antiterminator Q, thus leading to *stx* transcription. On the other hand, it was shown that the SOS response leads to de-repression of LEE2/3 promoter by activated RecA in a LexA-dependent manner in Enteropathogenic *E.coli*. Besides, a non-LEE phage encoded effector (*nleA*) also showed increased transcription in the presence of a DNA-damaging agent [56]. While we do not know the level of SOS induction during mouse colonization, this and the network of prophage regulators will affect expression of these colonization factors[7] .

In summary, *ler* over-expression led to a greater adhesion to intestinal epithelial cells *in vitro* and *in vivo*, together with reduced motility and enhanced Stx2 production. In contrast, adaptation of the 125RR strain to the mouse microenvironment led to multiple changes and differential regulation of virulence factors including TTSS up-regulation, improvement of *in vitro* and *in vivo* adhesion, increased acid resistance, increased FliC expression and motility, but decreased Stx2 production. Although *ler* over-expression did not reproduce some of the findings observed in the patho-adaptation of 125RR strain, this approximation allow us to conclude that an increased expression of TTSS proteins together with Stx expression resulted in a strain with increased colonization and pathogenicity *in vivo*.

Collectively, our findings illustrate the complex and variable nature of virulence gene expression in closely related isolates and the evolution of regulatory networks

associated with niche adaptation. The regulation of gene expression is in many cases very complex and involves multiple regulatory pathways, which could act synergistically or independently to adjust gene expression in response to specific environmental conditions and may be an important requirement for host adaptation. Besides, the mechanisms described herein may overlap with those supporting both ruminant to person and person-to-person transmission [61]. Understanding how host adaptation modulates the potential virulence of this pathogen is essential for delineating the pathogenesis of disease and may offer novel approaches to prevent and treat EHEC infection.

ACKNOWLEDGEMENTS

We would like to acknowledge Dr Angel Cataldi for generously providing Δ*stx* strain, and Vet Héctor Costa, Gabriela Camerano, Romina Fraiman, Edith Paxton and Jason Morgan for their excellent technical assistance.

CONFLICT OF INTEREST. The authors declare that they have no conflict of interest.

FUNDING. This work was supported by grants from BBSRC (UKRI) with an International Partnership Award BB/L026740/1; BBSRC Institute Strategic Programme Grant: Control of Infectious Diseases (BBS/E/D/20002173); Agencia Nacional de Promoción Científica y Tecnológica (APNCyT) Grant 278- 2016; Fundación Alberto J Roemmers 2015/2017; YCA was funded by the National Agency for Research and Development (ANID) /Scholarship Program / DOCTORADO BECAS CHILE/2016 - 72170349.

AUTHOR CONTRIBUTIONS. Data collection, formal analysis, investigation, methodology: RJFB, SPMA, JMC, YCA, JT; software, visualization, methodology: FF,

AB, SF, GP, MVR; conceptualization, resources, writing - original draft, writing - review & editing: RJFB, SPMA, SF, DLG, MSP; validation, supervision, funding acquisition, project administration: DLG, MSP.

REFERENCES

1. Griffin PM, Tauxe RV. The epidemiology of infections caused by Escherichia coli O157:H7, other enterohemorrhagic E. coli, and the associated hemolytic uremic syndrome. Epidemiol Rev. 1991;13:60-98.
2. Mahajan A, Currie CG, Mackie S, Tree J, McAteer S, McKendrick I, et al. An investigation of the expression and adhesin function of H7 flagella in the interaction of Escherichia coli O157 : H7 with bovine intestinal epithelium. Cell Microbiol. 2009;11(1):121-37.
3. Wolfson EB, Elvidge J, Tahoun A, Gillespie T, Mantell J, McAteer SP, et al. The interaction of Escherichia coli O157 :H7 and Salmonella Typhimurium flagella with host cell membranes and cytoskeletal components. Microbiology (Reading). 2020;166(10):947-65.
4. Tarr PI, Gordon CA, Chandler WL. Shiga-toxin-producing Escherichia coli and haemolytic uraemic syndrome. Lancet. 2005;365(9464):1073-86.
5. Tobe T, Beatson SA, Taniguchi H, Abe H, Bailey CM, Fivian A, et al. An extensive repertoire of type III secretion effectors in Escherichia coli O157 and the role of lambdoid phages in their dissemination. Proc Natl Acad Sci U S A. 2006;103(40):14941-6.
6. Fitzgerald SF, Beckett AE, Palarea-Albaladejo J, McAteer S, Shaaban S, Morgan J, et al. Shiga toxin sub-type 2a increases the efficiency of Escherichia coli O157 transmission between animals and restricts epithelial regeneration in bovine enteroids. PLoS Pathog. 2019;15(10):e1008003.
7. Tree JJ, Wolfson EB, Wang D, Roe AJ, Gally DL. Controlling injection: regulation of type III secretion in enterohaemorrhagic Escherichia coli. Trends Microbiol. 2009;17(8):361-70.
8. Elena SF, Lenski RE. Evolution experiments with microorganisms: the dynamics and genetic bases of adaptation. Nat Rev Genet. 2003;4(6):457-69.
9. Brzuszkiewicz E, Gottschalk G, Ron E, Hacker J, Dobrindt U. Adaptation of Pathogenic E. coli to Various Niches: Genome Flexibility is the Key. Genome Dyn. 2009;6:110-25.
10. Eriksson S, Bjorkman J, Borg S, Syk A, Pettersson S, Andersson DI, et al. Salmonella typhimurium mutants that downregulate phagocyte nitric oxide production. Cell Microbiol. 2000;2(3):239-50.
11. Silva WM, Dorella FA, Soares SC, Souza GH, Castro TL, Seyffert N, et al. A shift in the virulence potential of Corynebacterium pseudotuberculosis biovar ovis after passage in a murine host demonstrated through comparative proteomics. BMC Microbiol. 2017;17(1):55.
12. Bleich A, Kohn I, Glage S, Beil W, Wagner S, Mahler M. Multiple in vivo passages enhance the ability of a clinical Helicobacter pylori isolate to colonize the stomach of Mongolian gerbils and to induce gastritis. Lab Anim. 2005;39(2):221-9.
13. Chapuis E, Pages S, Emelianoff V, Givaudan A, Ferdy JB. Virulence and pathogen multiplication: a serial passage experiment in the hypervirulent bacterial insect-pathogen Xenorhabdus nematophila. PLoS One. 2011;6(1):e15872.
14. Fernandez H, Flores S, M PV, Medina G, Carrizo M. Enhancing adherence of Arcobacter butzleri after serial intraperitoneal passages in mice. Rev Argent Microbiol. 2013;45(2):75-9.

15. Liu X, Lu L, Pan C, Feng E, Wang D, Zhu L, et al. Comparative proteomics of Shigella flexneri 2a strain 301 using a rabbit ileal loop model reveals key proteins for bacterial adaptation in host niches. Int J Infect Dis. 2015;40:28-33.
16. Koskiniemi S, Gibbons HS, Sandegren L, Anwar N, Ouellette G, Broomall S, et al. Pathoadaptive mutations in Salmonella enterica isolated after serial passage in mice. PLoS One. 2013;8(7):e70147.
17. Fernandez-Brando RJ, Miliwebsky E, Mejias MP, Baschkier A, Panek CA, Abrey-Recalde MJ, et al. Shiga toxin-producing Escherichia coli O157 : H7 shows an increased pathogenicity in mice after the passage through the gastrointestinal tract of the same host. J Med Microbiol. 2012;61(Pt 6):852-9.
18. Elliott SJ, Sperandio V, Giron JA, Shin S, Mellies JL, Wainwright L, et al. The locus of enterocyte effacement (LEE)-encoded regulator controls expression of both LEE- and non-LEE-encoded virulence factors in enteropathogenic and enterohemorrhagic Escherichia coli. Infect Immun. 2000;68(11):6115-26.
19. Brando RJ, Miliwebsky E, Bentancor L, Deza N, Baschkier A, Ramos MV, et al. Renal damage and death in weaned mice after oral infection with Shiga toxin 2-producing Escherichia coli strains. Clin Exp Immunol. 2008;153(2):297-306.
20. Albanese A, Gerhardt E, Garcia H, Amigo N, Cataldi A, Zotta E, et al. Inhibition of water absorption and selective damage to human colonic mucosa induced by Shiga toxin-2 are enhanced by Escherichia coli O157:H7 infection. Int J Med Microbiol. 2015;305(3):348-54.
21. Wang RF, Kushner SR. Construction of versatile low-copy-number vectors for cloning, sequencing and gene expression in Escherichia coli. Gene. 1991;100:195-9.
22. Xu X, McAteer SP, Tree JJ, Shaw DJ, Wolfson EB, Beatson SA, et al. Lysogeny with Shiga toxin 2-encoding bacteriophages represses type III secretion in enterohemorrhagic Escherichia coli. PLoS Pathog. 2012;8(5):e1002672.
23. Gentleman RC, Carey VJ, Bates DM, Bolstad B, Dettling M, Dudoit S, et al. Bioconductor: open software development for computational biology and bioinformatics. Genome Biol. 2004;5(10):R80.
24. Gautier L, Cope L, Bolstad BM, Irizarry RA. affy--analysis of Affymetrix GeneChip data at the probe level. Bioinformatics. 2004;20(3):307-15.
25. Pearson RD, Liu X, Sanguinetti G, Milo M, Lawrence ND, Rattray M. puma: a Bioconductor package for propagating uncertainty in microarray analysis. BMC Bioinformatics. 2009;10:211.
26. Livak KJ, Schmittgen TD. Analysis of relative gene expression data using real-time quantitative PCR and the 2(-Delta Delta C(T)) Method. Methods. 2001;25(4):402-8.
27. Tree JJ, Roe AJ, Flockhart A, McAteer SP, Xu X, Shaw D, et al. Transcriptional regulators of the GAD acid stress island are carried by effector protein-encoding prophages and indirectly control type III secretion in enterohemorrhagic Escherichia coli O157:H7. Mol Microbiol. 2011;80(5):1349-65.
28. Letourneau J, Levesque C, Berthiaume F, Jacques M, Mourez M. In vitro assay of bacterial adhesion onto mammalian epithelial cells. J Vis Exp. 2011(51).
29. Lee J, Bansal T, Jayaraman A, Bentley WE, Wood TK. Enterohemorrhagic Escherichia coli biofilms are inhibited by 7-hydroxyindole and stimulated by isatin. Appl Environ Microbiol. 2007;73(13):4100-9.
30. Bak G, Han K, Kim D, Lee Y. Roles of rpoS-activating small RNAs in pathways leading to acid resistance of Escherichia coli. Microbiologyopen. 2014;3(1):15-28.
31. Council N. Guide for the care and use of laboratory animals. Washington DC: National Academies Press; 2011.
32. Keseler IM, Collado-Vides J, Gama-Castro S, Ingraham J, Paley S, Paulsen IT, et al. EcoCyc: a comprehensive database resource for Escherichia coli. Nucleic Acids Res. 2005;33(Database issue):D334-7.
33. Perna NT, Plunkett G, 3rd, Burland V, Mau B, Glasner JD, Rose DJ, et al. Genome sequence of enterohaemorrhagic Escherichia coli O157:H7. Nature. 2001;409(6819):529-33.
34. Battesti A, Majdalani N, Gottesman S. The RpoS-mediated general stress response in Escherichia coli. Annu Rev Microbiol. 2011;65:189-213.

35. Wang D, McAteer SP, Wawszczyk AB, Russell CD, Tahoun A, Elmi A, et al. An RNA-dependent mechanism for transient expression of bacterial translocation filaments. Nucleic Acids Res. 2018;46(7):3366-81.
36. Herold S, Siebert J, Huber A, Schmidt H. Global expression of prophage genes in Escherichia coli O157:H7 strain EDL933 in response to norfloxacin. Antimicrob Agents Chemother. 2005;49(3):931-44.
37. Lin J, Smith MP, Chapin KC, Baik HS, Bennett GN, Foster JW. Mechanisms of acid resistance in enterohemorrhagic Escherichia coli. Appl Environ Microbiol. 1996;62(9):3094-100.
38. Harrington CA, Rosenow C, Retief J. Monitoring gene expression using DNA microarrays. Curr Opin Microbiol. 2000;3(3):285-91.
39. Merrell DS, Hava DL, Camilli A. Identification of novel factors involved in colonization and acid tolerance of Vibrio cholerae. Mol Microbiol. 2002;43(6):1471-91.
40. Perry RD. Signature-tagged mutagenesis and the hunt for virulence factors. Trends Microbiol. 1999;7(10):385-8; discussion 8-9.
41. Hooda J, Shah A, Zhang L. Heme, an essential nutrient from dietary proteins, critically impacts diverse physiological and pathological processes. Nutrients. 2014;6(3):1080-102.
42. Gabbianelli R, Scotti R, Ammendola S, Petrarca P, Nicolini L, Battistoni A. Role of ZnuABC and ZinT in Escherichia coli O157:H7 zinc acquisition and interaction with epithelial cells. BMC Microbiol. 2011;11:36.
43. Callewaert L, Van Herreweghe JM, Vanderkelen L, Leysen S, Voet A, Michiels CW. Guards of the great wall: bacterial lysozyme inhibitors. Trends Microbiol. 2012;20(10):501-10.
44. Gaytan MO, Martinez-Santos VI, Soto E, Gonzalez-Pedrajo B. Type Three Secretion System in Attaching and Effacing Pathogens. Front Cell Infect Microbiol. 2016;6:129.
45. Frankel G, Phillips AD, Rosenshine I, Dougan G, Kaper JB, Knutton S. Enteropathogenic and enterohaemorrhagic Escherichia coli: more subversive elements. Mol Microbiol. 1998;30(5):911-21.
46. Paton AW, Voss E, Manning PA, Paton JC. Shiga toxin-producing Escherichia coli isolates from cases of human disease show enhanced adherence to intestinal epithelial (Henle 407) cells. Infect Immun. 1997;65(9):3799-805.
47. McNally A, Roe AJ, Simpson S, Thomson-Carter FM, Hoey DE, Currie C, et al. Differences in levels of secreted locus of enterocyte effacement proteins between human disease-associated and bovine Escherichia coli O157. Infect Immun. 2001;69(8):5107-14.
48. Beckham KS, Connolly JP, Ritchie JM, Wang D, Gawthorne JA, Tahoun A, et al. The metabolic enzyme AdhE controls the virulence of Escherichia coli O157:H7. Mol Microbiol. 2014;93(1):199-211.
49. Mellor GE, Fegan N, Gobius KS, Smith HV, Jennison AV, D'Astek BA, et al. Geographically distinct Escherichia coli O157 isolates differ by lineage, Shiga toxin genotype, and total shiga toxin production. J Clin Microbiol. 2015;53(2):579-86.
50. Olavesen KK, Lindstedt BA, Lobersli I, Brandal LT. Expression of Shiga toxin 2 (Stx2) in highly virulent Stx-producing Escherichia coli (STEC) carrying different anti-terminator (q) genes. Microb Pathog. 2016;97:1-8.
51. Iversen H, Lindback T, L'Abee-Lund TM, Roos N, Aspholm M, Stenfors Arnesen L. The gut bacterium Bacteroides thetaiotaomicron influences the virulence potential of the enterohemorrhagic Escherichia coli O103:H25. PLoS One. 2015;10(2):e0118140.
52. Tuttle J, Gomez T, Doyle MP, Wells JG, Zhao T, Tauxe RV, et al. Lessons from a large outbreak of Escherichia coli O157:H7 infections: insights into the infectious dose and method of widespread contamination of hamburger patties. Epidemiol Infect. 1999;122(2):185-92.
53. Small P, Blankenhorn D, Welty D, Zinser E, Slonczewski JL. Acid and base resistance in Escherichia coli and Shigella flexneri: role of rpoS and growth pH. J Bacteriol. 1994;176(6):1729-37.
54. Tramonti A, De Canio M, De Biase D. GadX/GadW-dependent regulation of the Escherichia coli acid fitness island: transcriptional control at the gadY-gadW divergent promoters and identification of four novel 42 bp GadX/GadW-specific binding sites. Mol Microbiol. 2008;70(4):965-82.

881 55. Tramonti A, Visca P, De Canio M, Falconi M, De Biase D. Functional characterization
882 and regulation of gadX, a gene encoding an AraC/XylS-like transcriptional activator of the
883 Escherichia coli glutamic acid decarboxylase system. J Bacteriol. 2002;184(10):2603-13.
884 56. Mellies JL, Barron AM, Carmona AM. Enteropathogenic and enterohemorrhagic
885 Escherichia coli virulence gene regulation. Infect Immun. 2007;75(9):4199-210.
886 57. Robinson CM, Sinclair JF, Smith MJ, O'Brien AD. Shiga toxin of enterohemorrhagic
887 Escherichia coli type O157:H7 promotes intestinal colonization. Proc Natl Acad Sci U S A.
888 2006;103(25):9667-72.
889 58. Iyoda S, Koizumi N, Satou H, Lu Y, Saitoh T, Ohnishi M, et al. The GrlR-GrlA
890 regulatory system coordinately controls the expression of flagellar and LEE-encoded type III
891 protein secretion systems in enterohemorrhagic Escherichia coli. J Bacteriol.
892 2006;188(16):5682-92.
893 59. Deng W, Puente JL, Gruenheid S, Li Y, Vallance BA, Vazquez A, et al. Dissecting
894 virulence: systematic and functional analyses of a pathogenicity island. Proc Natl Acad Sci U S
895 A. 2004;101(10):3597-602.
896 60. Wagner PL, Livny J, Neely MN, Acheson DW, Friedman DI, Waldor MK.
897 Bacteriophage control of Shiga toxin 1 production and release by Escherichia coli. Mol
898 Microbiol. 2002;44(4):957-70.
899 61. Rivas M, Chinen I, Miliwebsky E, Masana M. Risk Factors for Shiga Toxin-Producing
900 Escherichia coli-Associated Human Diseases. Microbiol Spectr. 2013;2(5).
901
902

903 **LEGENDS**

904 **Fig 1. Quantitative RT-PCR for selected genes.** Bacteria were cultured in MM9
905 media by triplicate until an $OD_{600}\approx0.9$. To calculate the relative expression ratio of the
906 genes of interest we used the $2^{-\Delta\Delta CT}$ method described previously [26]. The ribosomal
907 gene *rrsH* was used as reference.*$p<0.05$, t-test.

908 **Fig 2. Expression and functionality of TTSS proteins. (A) EspB/D protein**
909 **expression.** Bacteria were cultured in MM9 media until an $OD_{600}\approx0.9$ and supernatant
910 proteins were TCA-precipitated and separated through a 12% SDS-PAGE. Gels were
911 transferred onto nitrocellulose membranes to detect EspD (39.1 kDa) and RecA (38.0
912 kDa) proteins with specific antibodies as indicated. RecA in the whole cell fraction was
913 used as a growth control. A representative Western blot is shown out of three. **(B)**
914 **Western blot quantification.** Band intensities were quantified by using the ImageJ
915 program as detailed in the Methods section. The intensity is expressed as Arbitrary
916 Units. EspD/RecA mean ± SEM from three repeats is shown.***$p<0.001$, t-test (**C)**

Adherence to Caco-2 and HCT-8 intestinal epithelial cells. Bacterial suspensions of 125/99 and 125RR strains in MM9 media were added by triplicate to semiconfluent monolayers of Caco-2 and HCT-8 cell cultures (MOI≈5 or 20 respectively). Adherent bacteria were determined by counting the number of CFU that had adhered to epithelial cells after 4 h incubation. Results are expressed as the mean percentage relative to the amount of seeded bacteria ± SEM. One representative experiment out of at least three with similar results is shown. Two-way ANOVA $p<0.001$, Bonferroni post-test *$p<0.05$, **$p<0.01$. (**D) Confocal images of Caco-2 and HCT-8 cells infected with 125/99 and 125RR strains.** Bacteria were grown in MM9 for 2 h. After 5 h of infection, cells were fixed in 4% PFA. Bacteria were stained with anti-O157 and Alexa Fluor 488-conjugated secondary antibody, nuclei with ToPro 3-iodide, and actin polymerization with PhalloidiniFluor-555. Representative images are shown. Magnification 60X. (**E) Bacterial area per cell nucleus.** Confocal images were analyzed automatically as indicated in Methods section. Results are shown as bacterial area per nucleus of epithelial cell. Two slides per treatment and five fields per slide were analyzed. Two-way ANOVA *$p<0.05$.

Fig 3. Other virulence traits. (A) and (B) Swimming-motility on soft-agar plates. Overnight cultures of 125/99 and 125RR in MM9 media were used. Motility was measured in a 24 and 48 h soft agar swimming assay. **(A)** Representative plates. The motility is visualized as halos of radial diffusion of bacteria around the primary inoculum. **(B)** Results are expressed as motility diameter (mm) means ± SEM. A representative experiment out of four is shown. Two-way ANOVA: strain $p<0.05$, time $p<0.01$; Bonferroni: **$p<0.01$. **(C) Quantification of Stx2 production by ELISA**. 125/99 and 125RR strain were cultured for 4 h and overnight (ON) as indicated, and Stx2 concentration was measured on the supernatant by ELISA. Δ*stx* was used as a

942 negative control. Two-way ANOVA: time $p<0.001$, bacterial strain $p<0.05$; Bonferroni:
943 ***$p<0.001$.Values are averaged from two independent cultures. Experiment was
944 repeated three times. **(D) and (E) Acid resistance of 125/99 and 125RR strains.**
945 Survival rates of stationary-phase bacteria after exposure to pH 2.5 for **(D)** 1 or **(E)** 2 h
946 were determined. ON cultures were carried out in MM9 media supplemented with 0.4
947 % glucose for all the conditions except AR0, in which 0.4 % glycerol was used. The
948 following day a 1/10 dilution was carried out on stress acid media. This media consisted
949 of MM9 supplemented with 0.4 % glucose in AR0, and 1.5 mM glutamate in AR1 or
950 0.6 mM arginine in AR2. Controls were exposed to the same media at pH 2.5 the
951 following day. Values are averaged from two independent cultures. A representative
952 experiment out of three is shown. **(D)** Two-way ANOVA: bacterial strain $p<0.05$; AR
953 system $p<0.0001$**. (E)** Two-way ANOVA: Bacterial strain $p<0.0001$; AR system
954 $p<0.0001$; Bonferroni: ***$p<0.001$.

955 **Fig 4. *ler* over-expression in *trans*. (A) EspB/D protein expression.** Transformed
956 bacteria were cultured in MEM-HEPES medium supplemented with 200 µg/mL
957 ampicillin, glucose and Fe^{3+} for 1 h when 1 mM of IPTG was added and bacteria were
958 grown until an $OD_{600}\approx0.9$. Culture supernatant proteins were TCA precipitated and
959 separated through a 12 % SDS-PAGE. Gels were stained with colloidal blue or
960 transferred onto nitrocellulose membranes to detect EspD and RecA proteins with
961 specific antibodies as indicated. RecA was used as a load control. A representative
962 image is shown **(B) Adherence to Caco-2 intestinal epithelial cells.** Semiconfluent
963 monolayers of Caco-2 cells were infected with the indicated bacteria at an MOI≈10 and
964 the number of CFU that adhered to cells after 3 h incubation was determined. Results
965 are expressed as the mean percentage relative to the amount of seeded bacteria ± SEM.
966 A representative experiment out of three is shown. Two-way ANOVA bacterial strain

967 p<0.0001, epithelial cell line p<0.0001; Bonferroni:**p<0.01, ***p<0.001. **(C) (D)**
968 **Confocal images of Caco-2 cells infected with bacterial strains.** After 3 h of
969 infection, cells were fixed in 4 % PFA. Bacteria were stained with anti-O157 and Alexa
970 Fluor 488-conjugated secondary antibody, nuclei with ToPro 3-iodide, and actin
971 polymerization with PhalloidiniFluor-555. Representative images are shown.
972 Magnification 60x **(C)**, zoomed-images 300x **(D)**. **(E) Bacterial area per cell nucleus.**
973 Automated Image Analysis was carried out as indicated in Methods section. Two slides
974 per treatment and five fields per slide were analyzed. One-way ANOVA p<0.0001;
975 Bonferroni: **p<0.01, ***p<0.001. **(F) Swimming-motility on soft-agar plates.**
976 Motility was measured as the halos of radial diffusion from the primary inoculum in
977 soft agar plates at 48 h. Results are expressed as motility diameter (mm) means ± SEM.
978 A representative experiment out of three with similar results is shown. ANOVA
979 p<0.0001; Bonferroni: *p<0.05 ***p<0.001. **(G) Quantification of Stx2 production**
980 **by ELISA**. Stx-producing strains (125/99 pWSK*ler* and 125/99 pWSK29) were
981 cultured for 1 h and 1 mM IPTG was added in order to induce *ler* production. Aliquots
982 were withdrawn at 0, 3 and 3.5 h of *ler* induction and Stx2 concentration was measured
983 on the supernatant by ELISA. A representative experiment out of three with similar
984 results is shown. Two-way ANOVA, bacterial strain p< 0.01; time of induction
985 p<0.001; Bonferroni ***p<0.001.

986 **Fig 5. *ler* over-expression increase pathogenicity *in vivo*. (A) Mice survival.** Mice at
987 weaning (125/99 pWSK*ler* n:10; 125/99 pWSK29 n:10; Δ*stx* pWSK*ler* n:6; Δ*stx*
988 pWSK29 n:4) were intra-gastrically infected with 10^{12} CFU/kg of the indicated strain.
989 Survival was monitored daily. Log-rank Test **p<0.01. **(B) Plasmatic urea levels.**
990 Mice were bled at 96 h after infection and urea levels were determined. One-Way
991 ANOVA: p<0.001, Bonferroni: ***p<0.001. **Bacterial isolation from feces (C), small**

(D) and large (E) intestine. Mice were killed at 96 h after intra-gastric inoculation of the indicated bacterial strains and the number of CFU was determined in feces and intestines as described in Methods. Five to six animals per experimental group were analyzed. Two-Way ANOVA: $p<0.0001$; Bonferroni *$p<0.05$, **$p<0.01$, ***$p<0.001$.

Supporting information

S1Table. Microarray analysis of genes differentially transcribed on stool-recovered strain (125RR) compared to wild type strain (125/99).

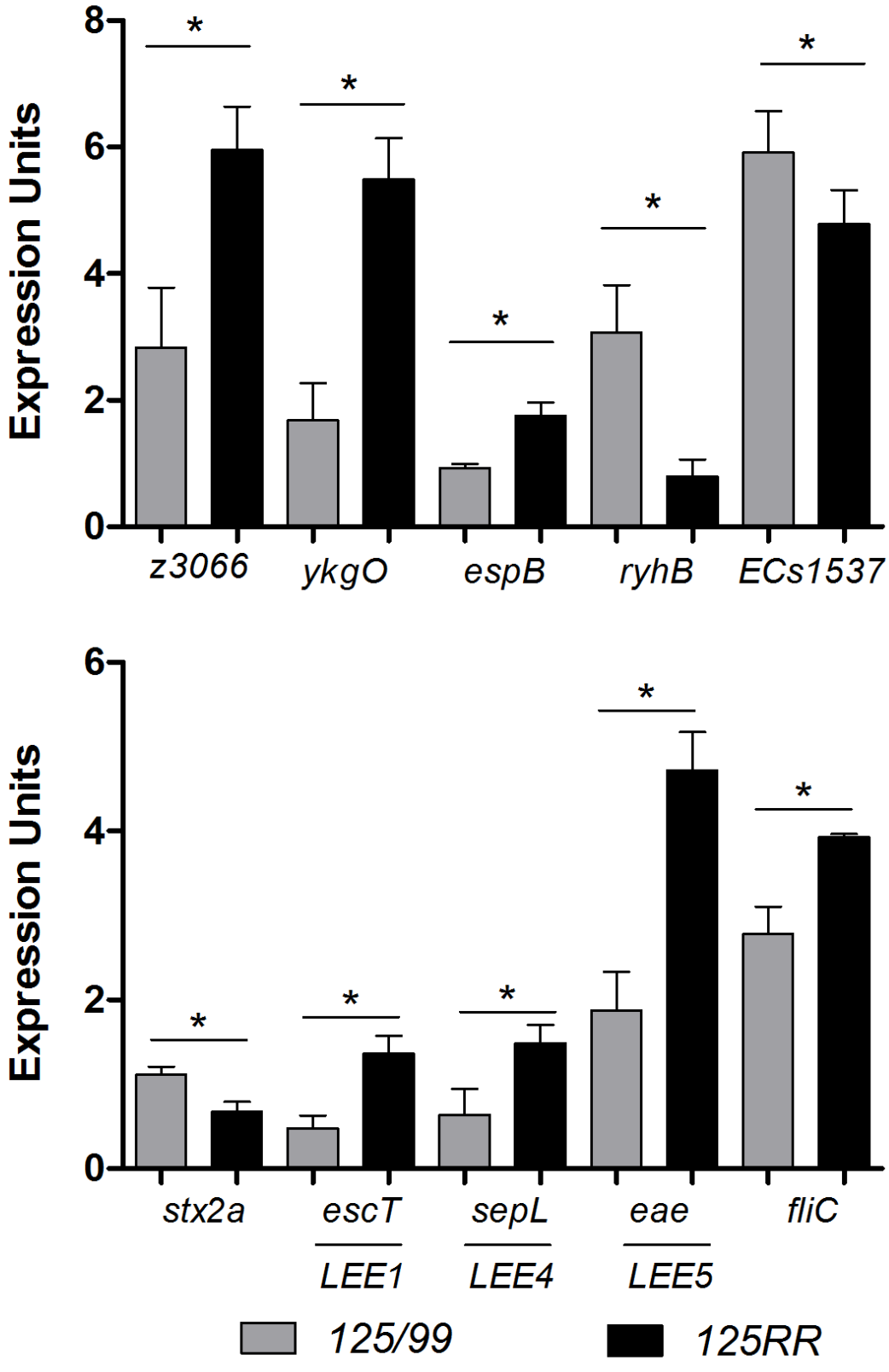
Expression Units
8
6
4
2
0
*
*
*
*
*
z3066
ykgO
espB
ryhB
ECs1537
Expression Units
6
4
2
0
*
*
*
*
*
stx2a
escT
sepL
eae
fliC
LEE1
LEE4
LEE5
125/99
125RR

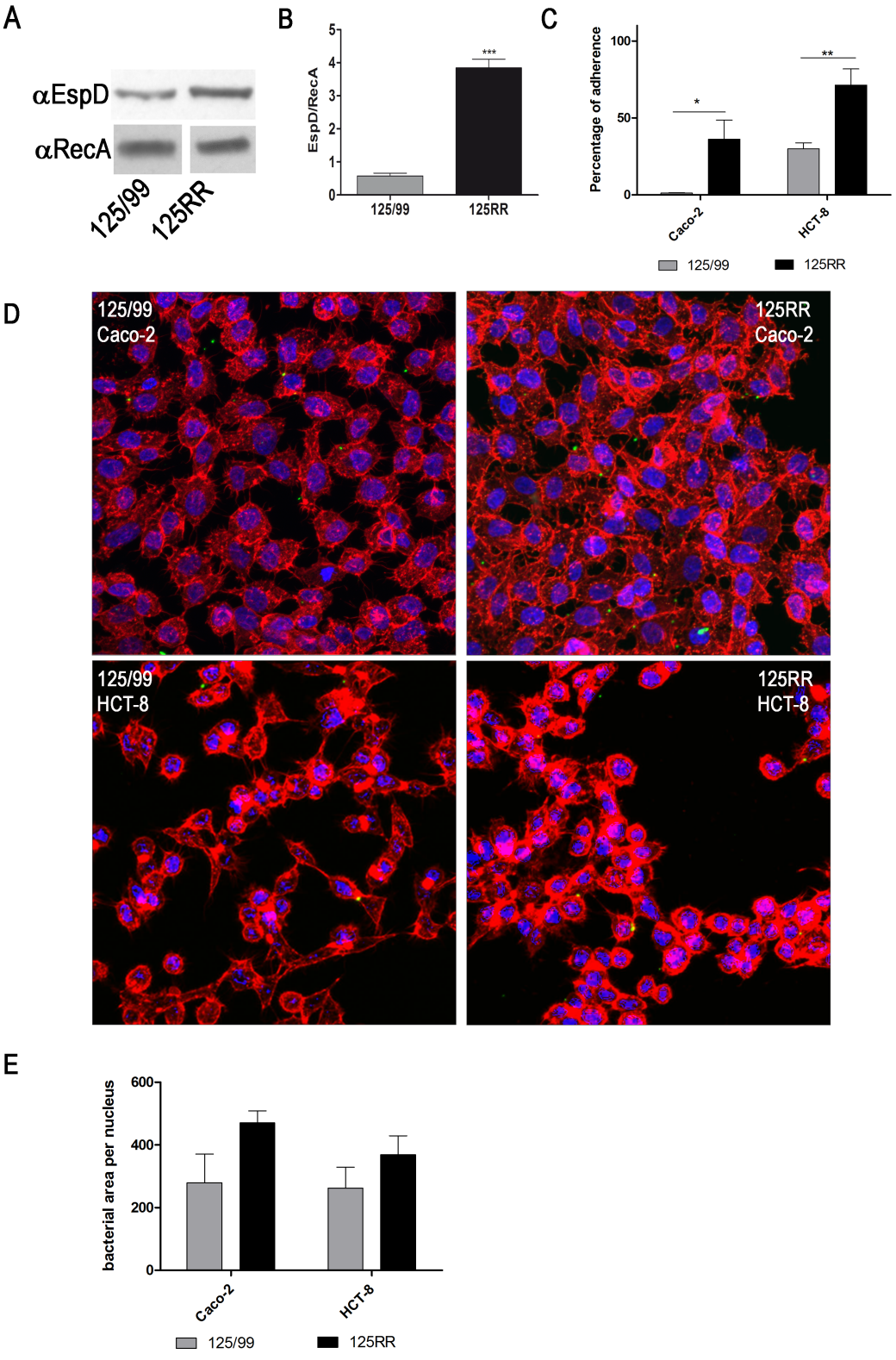
A
αEspD
αRecA
125/99
125RR
B
EspD/RecA
***
125/99
125RR
C
Percentage of adherence
*
**
Caco-2
HCT-8
125/99
125RR
D
125/99
Caco-2
125RR
Caco-2
125/99
HCT-8
125RR
HCT-8
E
bacterial area per nucleus
Caco-2
HCT-8
125/99
125RR

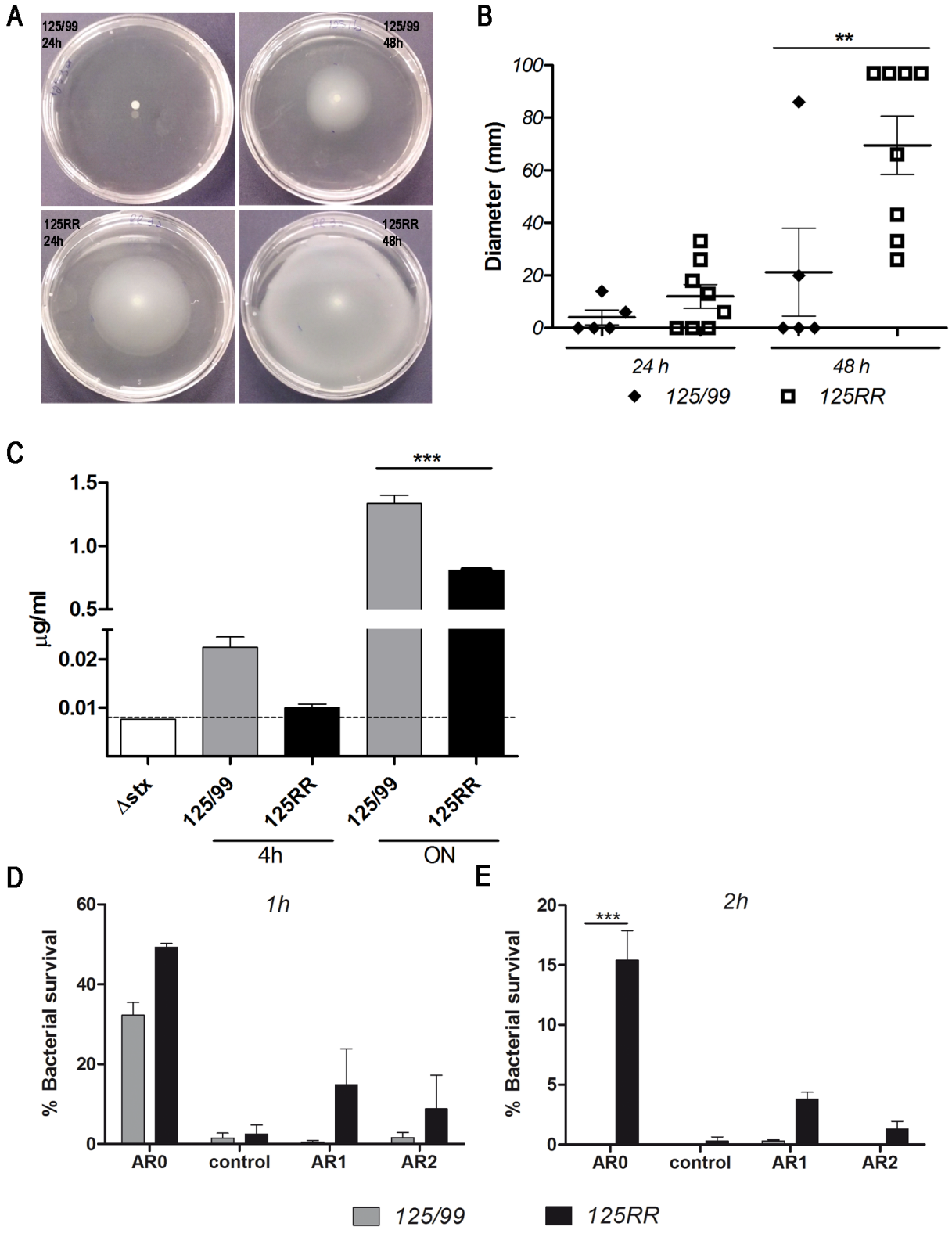
A
125/99
24h
125/99
48h
125RR
24h
125RR
48h
B
**
Diameter (mm)
100
80
60
40
20
0
24 h
48 h
125/99
125RR
C
***
µg/ml
1.5
1.0
0.5
0.02
0.01
Δstx
125/99
125RR
125/99
125RR
4h
ON
D
1h
% Bacterial survival
60
40
20
0
AR0
control
AR1
AR2
E
2h
***
% Bacterial survival
20
15
10
5
0
AR0
control
AR1
AR2
125/99
125RR

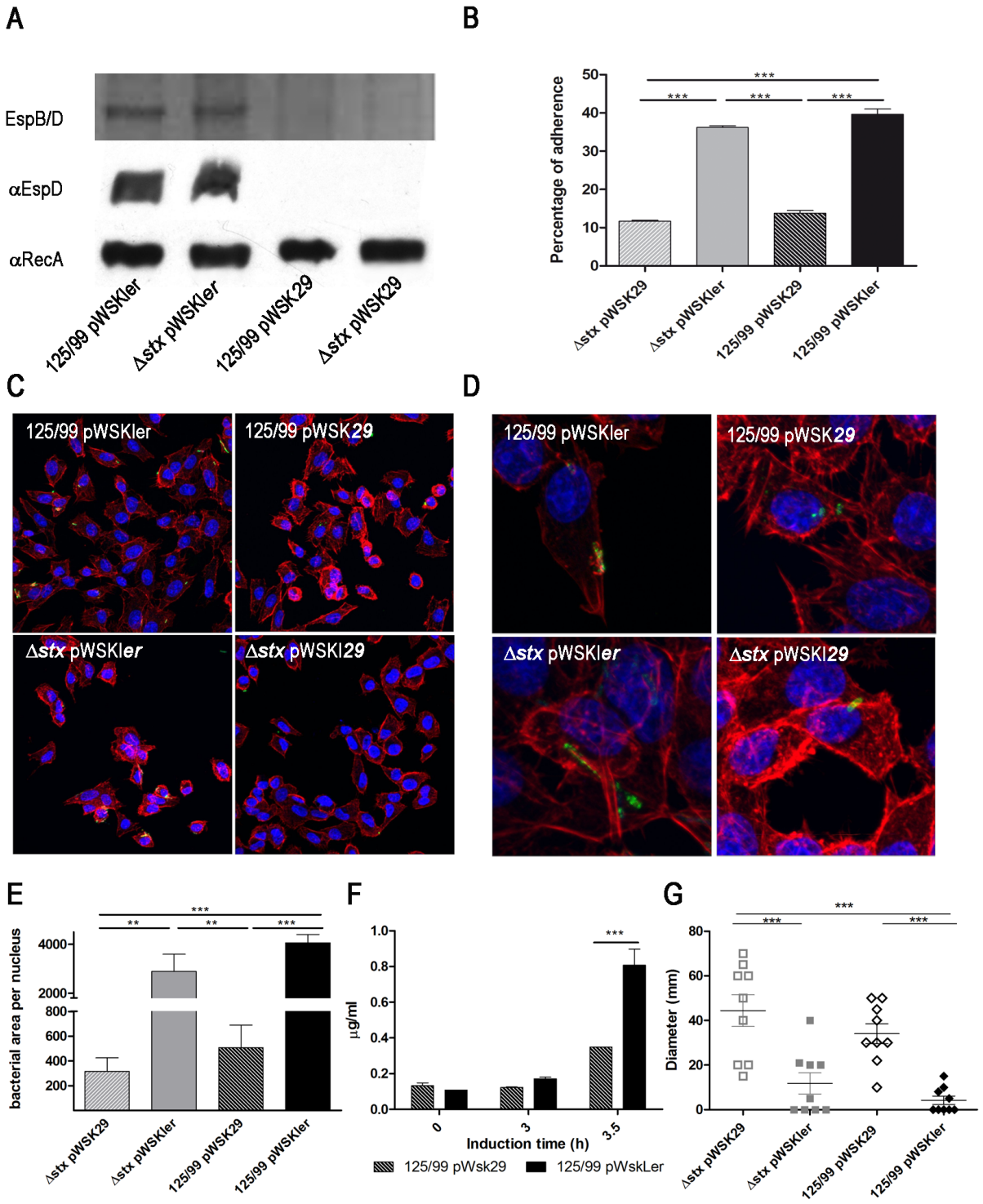
A
EspB/D
αEspD
αRecA
125/99 pWSKler
Δstx pWSKler
125/99 pWSK29
Δstx pWSK29
B
Percentage of adherence
50
40
30
20
10
0
***
***
***
***
Δstx pWSK29
Δstx pWSKler
125/99 pWSK29
125/99 pWSKler
C
125/99 pWSKler
125/99 pWSK29
Δstx pWSKler
Δstx pWSKl29
D
125/99 pWSKler
125/99 pWSK29
Δstx pWSKler
Δstx pWSKl29
E
bacterial area per nucleus
4000
2000
800
600
400
200
**
**
***
***
Δstx pWSK29
Δstx pWSKler
125/99 pWSK29
125/99 pWSKler
F
µg/ml
1.0
0.8
0.6
0.4
0.2
0.0
***
0
3
3.5
Induction time (h)
125/99 pWsk29
125/99 pWskLer
G
Diameter (mm)
80
60
40
20
0
***
***
***
Δstx pWSK29
Δstx pWSKler
125/99 pWSK29
125/99 pWSKler

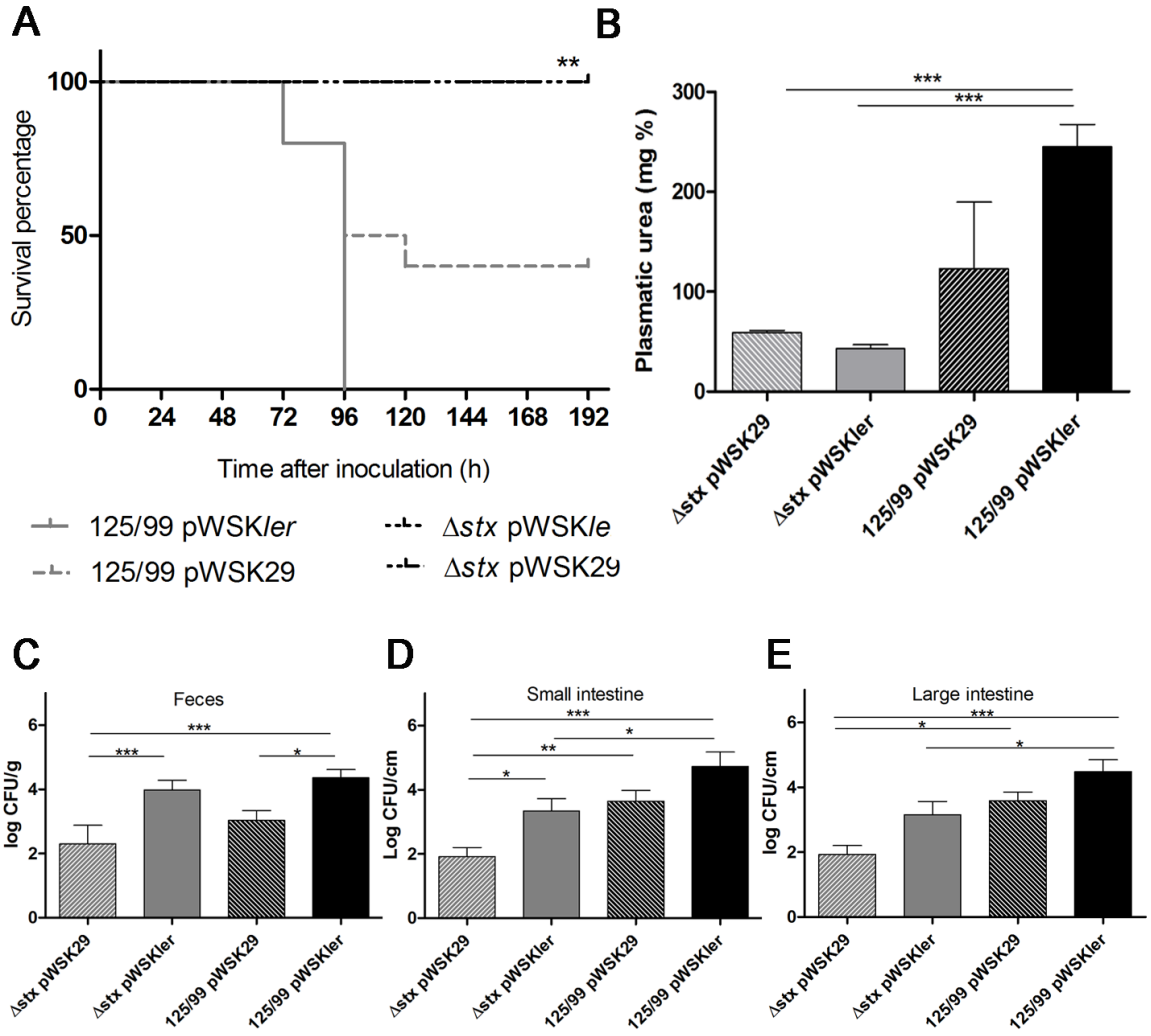
A
B
Survival percentage
100
50
0
0 24 48 72 96 120 144 168 192
Time after inoculation (h)
**
125/99 pWSKler
125/99 pWSK29
Δstx pWSKler
Δstx pWSK29
Plasmatic urea (mg %)
300
200
100
0
***
***
Δstx pWSK29
Δstx pWSKler
125/99 pWSK29
125/99 pWSKler
C
D
E
Feces
log CFU/g
Small intestine
Log CFU/cm
Large intestine
log CFU/cm
6
4
2
0
*
**
***